Published in "Biomaterials 172: 105–115, 2018"
which should be cited to refer to this work.

Engineered hybrid spider silk particles as delivery system for peptide vaccines

Matthias Lucke [a, e, 1], Inès Mottas [b, c, h, 1], Tina Herbst [b], Christian Hotz [b], Lin Römer [f], Martina Schierling [d], Heike M. Herold [d], Ute Slotta [f], Thibaud Spinetti [b], Thomas Scheibel [d, 2], Gerhard Winter [a, 2], Carole Bourquin [b, c, g, h, **, 2], Julia Engert [a, *, 2]

[a] Department of Pharmacy, Pharmaceutical Technology & Biopharmaceutics, Ludwig-Maximilians-University Munich, Butenandtstrasse 5, 81377 Munich, Germany
[b] Department of Medicine, Faculty of Science, University of Fribourg, Chemin Du Musée 5, 1700 Fribourg, Switzerland
[c] Ecole de Pharmacie Genève-Lausanne, University of Geneva, Rue Michel-Servet 1, 1211 Geneva, Switzerland
[d] University of Bayreuth, Faculty of Engineering Science, Chair for Biomaterials, Universitätsstrasse 30, 95440 Bayreuth, Germany
[e] Coriolis Pharma, Fraunhoferstrasse 18B, 82152 Planegg/Martinsried, Germany
[f] AMSilk GmbH, Am Klopferspitz 19, 82152 Planegg/Martinsried, Germany
[g] Department of Anesthesiology, Pharmacology and Intensive Care, Faculty of Medicine, University of Geneva, Rue Michel-Servet 1, 1211, Geneva, Switzerland
[h] Ecolede Pharmacie Genève-Lausanne, University of Lausanne, Rue Michel-Servet 1, 1211 Geneva, Switzerland

The generation of strong T-cell immunity is one of the main challenges for the development of successful vaccines against cancer and major infectious diseases. Here we have engineered spider silk particles as delivery system for a peptide-based vaccination that leads to effective priming of cytotoxic T-cells. The recombinant spider silk protein eADF4(C16) was fused to the antigenic peptide from ovalbumin, either without linker or with a cathepsin cleavable peptide linker. Particles prepared from the hybrid proteins were taken up by dendritic cells, which are essential for T-cell priming, and successfully activated cytotoxic T-cells, without signs of immunotoxicity or unspecific immunostimulatory activity. Upon subcutaneous injection in mice, the particles were taken up by dendritic cells and accumulated in the lymph nodes, where immune responses are generated. Particles from hybrid proteins containing a cathepsin-cleavable linker induced a strong antigen-specific proliferation of cytotoxic T-cells in vivo, even in the absence of a vaccine adjuvant. We thus demonstrate the efficacy of a new vaccine strategy using a protein-based all-in-one vaccination system, where spider silk particles serve as carriers with an incorporated peptide antigen. Our study further suggests that engineered spider silk-based vaccines are extremely stable, easy to manufacture, and readily customizable.

Keywords:
Vaccine delivery
Antigen delivery
Peptide vaccines
Cytotoxic T-cells
Recombinant silk protein

1. Introduction

Vaccination prevents the spread of many deadly infectious diseases, and it is considered to be one of the most effective interventions for global health ever developed [1]. The protective effect of vaccines is essentially due to B lymphocyte production of neutralizing antibodies against infectious agents or toxins. Although in many infectious diseases this humoral immunity is of major importance, in some cases cellular immunity is essential for protection [2]. Indeed, cytotoxic T-cells, the main effector cells of cellular immunity, are required for the development of successful immune responses against chronic infections such as HIV, malaria

* Corresponding author. Department of Pharmacy, Pharmaceutical Technology & Biopharmaceutics, Ludwig-Maximilians-University Munich, Butenandtstrasse 5, 81377 Munich, Germany
** Corresponding author. Ecole de Pharmacie Genève-Lausanne, University of Geneva, Rue Michel-Servet 1, 1211 Geneva, Switzerland.
E-mail addresses: carole.bourquin@unige.ch (C. Bourquin), julia.engert@cup.uni-muenchen.de (J. Engert).
[1] First authors equal contribution: Matthias Lucke and Inès Mottas contributed equally to this work.
[2] Senior authors equal contribution: Thomas Scheibel, Gerhard Winter, Carole Bourquin and Julia Engert contributed equally to this work.

or tuberculosis [3]. Furthermore, recent studies have shown that T-cell-mediated immunity can lead to cancer regression in patients, even in the case of advanced disease [4]. Unfortunately, most current vaccination strategies do not induce effective cytotoxic T-cell responses and the development of vaccines that promote cellular immunity thus remains a major challenge [5].

The initiation of cytotoxic T-cell responses requires the priming of naïve $CD8^+$ T-cells by professional antigen-presenting cells such as dendritic cells [6,7]. Dendritic cells are located in many tissues and constantly sample their surroundings. When these cells encounter microbes or particulate matter, or indeed vaccination-delivered antigens, these are engulfed and processed in order to cross-present antigenic peptides to T-cells via major histocompatibility complex class I molecules (MHC I) [8,9]. To induce effective immunity, immature dendritic cells must be activated by specific maturation signals [10]. For this reason, in addition to microbial antigens, most vaccines include adjuvants that stimulate dendritic cell maturation and thus the generation of cytotoxic T-cell immunity [11,12]. The maturation of dendritic cells occurs during their migration from peripheral tissues to the lymph nodes [13]. In the lymph nodes, $CD8^+$ T-cells are primed by direct contact with mature dendritic cells presenting their cognate antigen [14]. Primed T-cells proliferate in the lymph nodes and differentiate to effector cytotoxic T-cells that patrol the body to kill infected or tumoral cells.

The elucidation of the amino acid sequences of microbial or tumor-associated antigens has led to the development of peptide vaccination [15]. Vaccines comprised of antigenic peptides instead of full-length proteins activate only the cytotoxic T-cells that recognize disease-specific epitopes, thus limiting the risk of unspecific autoimmune toxicity. However, peptide vaccination has shown limited success due to several factors. First, peptides are rapidly degraded by proteases: the MelanA/MART-1 tumor antigenic peptide for instance is degraded in 22 s in plasma [16]. Second, peptides can bind to MHC I not only on antigen-presenting cells but on all nucleated cells, thus promoting tolerance rather than immunity [17,18]. Furthermore, to be effective the vaccine peptides must form a stable complex with MHC I molecules during dendritic cell migration to the lymph node [19,20], which takes approximatively 18 h [21]. To meet these challenges, antigens can be protected by particulate carriers. Particle delivery systems can limit peptide degradation, improve uptake of antigen by dendritic cells [22] and ensure that the antigen is processed intracellularly before loading onto MHC I [23].

For the design of particle-based delivery systems, antigen can be coupled to the particles by different methods [24]. The antigen may be adsorbed to the surface of the particle, as is the case with aluminum-based formulations [25]. However, binding by non-covalent interactions may result in rapid antigen release from the carrier upon changes in pH. The antigen can also be encapsulated in a polymer matrix during manufacturing, but this may damage protein-based antigens due to the relatively harsh conditions commonly applied during particle preparation [26]. Chemical conjugation of the antigen to the carrier bears the risk of losing certain epitopes during conjugation [27]. To circumvent these difficulties, we chose to use a protein-based carrier and directly incorporated the antigenic peptide into the sequence of the carrier protein derived from spider silk. Spider silk protein is a promising material, because previous studies demonstrated that the protein itself is poorly immunogenic and does not cause inflammatory reactions in rats [28,29]. Indeed, in addition to their clear advantage in terms of biocompatibility and biodegradability, spider silk particles allow for solvent-free synthesis and steam sterilization [30,31].

2. Materials and methods

2.1. Preparation of spider silk hybrid proteins

eADF4(C16) is based on 16 repeats of the consensus sequence of spidroin ADF4 of the European garden spider (Araneus diadematus) (C-module: GSSAAAAAAAASGPGGY GPENQGPSGPG-GYGPGGPG), and a T7-tag fused to the amino terminus for detection purposes [32]. $OVA_{257\text{-}264}$ peptide (SIINFEKL) was fused to the eADF4(C16) by either using a cathepsin B cleavable linker (GFLG) or a cathepsin S cleavable linker (PMGLP). Fusions were made using tags and DNA sequences of the tags were inserted into the cloning vector pCS of eADF4(C16) by seamless cloning as described previously [31,32]. The resulting constructs and the modified proteins are shown in Fig. S1. Successful cloning was confirmed by sequencing.

2.2. Preparation of spider silk hybrid particles

Preparation of spider silk hybrid particles was performed using the well-established preparation technique using a micromixing system as described before [33]. Briefly, spider silk protein powders were dissolved in a 6 M guanidinium thiocyanate solution and subsequently dialyzed against a 10 mM Tris/HCl solution. The dialyzed solution was 0.2 μm filtered before particle preparation. The particle preparation was subsequently conducted by mixing pretempered spider silk protein solution (1 mg/ml) with either a pretempered 2 M potassium phosphate solution or 2–4 M ammonium sulfate solution. Resulting spider silk particles were washed with highly purified water (HPW) three times followed by a two-minute ultrasonication treatment.

2.2.1. Preparation of spider silk hybrid particles for in vitro and in vivo studies

The before mentioned particle preparation process was slightly adjusted for particles used during in vitro and in vivo experiments. Prior to dissolution in 6 M guanidinium thiocyanate the spider silk powder was suspended in HPW and steam sterilized for 15 min at 121 °C. In addition, chemicals with low endotoxin levels were used throughout the whole preparation process. Endotoxin content of the protein solution was determined using an Endosafe-PTS reader (Charles River Laboratories, Wilmington, USA) after a 20–40-fold dilution with HPW.

2.3. Particle sterilization

Suspensions of spider silk particles were sterilized by autoclave treatment in a GTA 50 autoclave (Fritz Gössner, Hamburg, Germany) as described before [34]. All spider silk particles were suspended in highly purified water at a concentration of 1 mg/ml. Sterilization was performed for 15 min at 121 °C.

2.4. Fluorescent labelling

Labelling of spider silk protein with fluorescein isothiocyanate (FITC) was performed based on the published method by Spieß et al. using the terminal amine group of the spider silk protein [30]. For the preparation of fluorescently labeled particles used for in vivo studies, an endotoxin-free 20 mM HEPES solution instead of a 10 mM Tris/HCl solution was used for dialysis to facilitate the coupling of FITC. After dialysis, a 20-fold molar excess of FITC (dissolved in DMSO) was added slowly to the spider silk solution followed by a 3 h incubation in the dark. The FITC-coupled spider silk protein solution was used for particle preparation as described before. The fluorescent labelling of particles used for in vitro studies

only was carried out at pre-prepared particles. Spider silk particles were suspended at a concentration of 2.5 mg/ml in an endotoxin-free 20 mM HEPES buffer. A 20-fold molar excess of FITC (dissolved in DMSO) was added dropwise to the particle suspension. After incubation for 72 h in the dark, the particles were centrifuged and washed with HPW for three times. Additional ultrasonication for 2 min completed the preparation process.

2.5. Release of OVA peptide from hybrid spider silk particles by cathepsin cleavage

The C16-catSsub-OVAp particles were suspended to a final concentration of 2 mg/ml with a 50 mM sodium acetate buffer, pH 5.5, containing 1 mM EDTA and 2 mM DTT. To this suspension, 0.9 mU/ml (5 ng/μl) cathepsin S was added for incubation at 37 °C [35]. As suggested by Calbiochem, the pH of the before mentioned acetate buffer was adjusted to 5.0 for incubation with cathepsin B enzyme. 0.1 U/ml (0.36 ng/μl) cathepsin B was added to C16-catBsub-OVAp particles for incubation at 37 °C [36]. Samples were drawn after 1, 6, 24, 48, 72 and 96 h incubation time and analyzed by RP-HPLC. To do so, the sample supernatant was separated by a Waters 2695 module (Waters Corporation, Milford, MA, USA) equipped with a reversed phase YMC-Triart C18 column (YMC Europe GmbH, Dinslaken, Germany). Peptide detection was carried out at 220 nm on a Waters UV−Vis detector 2487 (Waters Corporation, Milford, MA, USA). Peptides with the predicted cleavage sequence were used for standard curves. The cleavage sites of the linkers had been described in literature earlier [35,37,38]. The peptide IGSIINFEKLG was used for evaluation of C16-catBsub-OVAp protein and the peptide LPGSIINFEKLG was used for evaluation of C16-catSsub-OVAp protein, respectively. Data analysis was performed using Chromeleon 6.80 software (Dionex GmbH, Germering, Germany).

2.6. Dynamic light scattering (DLS)

Particle size and size distribution of submicroparticles were measured in triplicate by dynamic light scattering (DLS) using a Zetasizer Nano ZS (Malvern Instruments, Worcestershire, UK). Particle size is provided as the Z-average value, and the particle size distribution is displayed by the polydispersity index (PDI). Directly before each measurement, samples were diluted to a final concentration of 0.01 mg/ml with HPW. All measurements were conducted at 25 °C.

2.7. Zeta potential

The zeta potential of spider silk particles was measured using a disposable capillary cell (DTS1061, Malvern Instruments, Worcestershire, United Kingdom) in a Zetasizer Nano ZS (Malvern Instruments, Worcestershire, United Kingdom). The spider silk particle samples were diluted to 0.05 mg/ml with freshly prepared 20 mM sodium chloride (NaCl) solution for analysis [33,39]. The measurements were conducted in triplicate at 25 °C.

2.8. Scanning electron microscopy (SEM)

For SEM imaging, small droplets of spider silk particle suspensions were placed onto Thermanox® plastic cover slips (Nunc, Rochester, USA). The spider silk particle suspensions were dried and carbon sputtered under vacuum at room temperature. Analysis was performed using a Joel JSM-6500F microscope (Joel Inc., Peabody, USA) at magnifications of 20,000×.

2.9. Mice

Female C57BL/6JRj mice (Janvier Labs, Roubaix, France) and OT-I mice (C57BL/6-Tg (TcraTcrb)1100Mjb/Crl; Charles River, Wilmington, USA) were housed under specific pathogen-free conditions and used at 6−12 weeks of age. Animal experimentation was conducted according to Swiss regulations.

2.10. Cell culture

Bone marrow-derived dendritic cells (BMDC) and single-cell suspensions of primary splenocytes were prepared as described [40], plated in flat-bottom 96-well plates ($5x10^4$ cells/well) and exposed to spider silk particles at a working concentration of 50 μg/ml (= 1 μg OVA peptide/ml) except for cytotoxicity testing (500 μg/ml). At 500 μg/ml, particles did not interfere with ELISA or flow cytometry reading [41]. OVA peptide (1 μg/ml) was used as control. Staurosporine (1 nM) (Sigma-Aldrich, Saint Louis, USA) was used as positive control to induce apoptosis (not shown). Lipopolysaccharide (LPS) (100 ng/ml) and resiquimod (R848; 0.25 μg/ml) (both from Invitrogen, Carlsbad, USA) were used as adjuvant to induce BMDC maturation. After 24 h particle exposure, cells were harvested for flow cytometry analysis, and the supernatant was stored at −20 °C for cytokine quantification.

2.11. Flow cytometry

Flow cytometry analysis was performed with a MACSquant analyzer 10 (Miltenyi Biotec, Bergisch Gladbach, Germany). To assess cell viability, BMDC were incubated with annexin V-APC (Biolegend, San Diego, USA) according to the manufacturer's instructions. Propidium iodide (Sigma-Aldrich, Saint Louis, USA) was automatically added by the MACSquant analyzer before analysis. For other flow cytometry measurements, cells were stained with zombie violet dye (Biolegend, San Diego, USA) to exclude dead cells and washed with FACS buffer consisting of PBS (Eurobio, Les Ulis, France) supplemented with 2 mM EDTA (Calbiochem, San Diego, USA) and 0.5% BSA (PAA laboratories, Austria). Fc receptors were blocked by incubation with anti-mouse unlabeled CD16/32 (Biolegend, San Diego, USA) for 10 min at 4 °C before addition of anti-mouse labeled antibodies for further 30 min at 4 °C: APC-Cy7-MHC II/I-A/I-E (M5/114.15.2), PB-CD3 (17A2), APC-Cy7-CD8 (53−6.7), PerCP-B220/CD45R (RA3-6B2), Pe-Cy7-Cd11c (N418), APC-CD11b (M1/70), APC-CD11c (N418) (all from Biolegend) and APC-MCH-I/H.2Kb (AF6-88.5.5.3) (ebioscience, San Diego, USA). Corresponding isotype controls were used (data not shown). The cells were washed once and resuspended in FACS buffer before acquisition. BMDC were defined as $CD11c^+$ cells. The following splenocyte subpopulations were defined: T-cells ($CD3^+B220^-$), dendritic cells ($CD3^-B220^-CD11c^+$) and macrophages/monocytes ($CD3^-B220^-CD11c^-CD11b^+$). Data were analyzed using FlowJo software version 9.9.4 (FlowJo Analysis software, Ashland, USA).

2.12. 3-(4,5-Dimethylthiazol-2-yl)-2,5-diphenyltetrazolium bromide (MTT) assay

The vybrant MTT cell proliferation assay kit (Molecular Probes, Eugene, USA) was used according to the manufacturer's protocol. MTT was added to BMDC after 24 h of particle exposure. For this assay, complete BMDC medium without phenol red (Bio West, Nuaillé, France) was used.

2.13. Analysis of cytokine production by ELISA

ELISA Max deluxe sets for mouse IL-6, TNF-α and IFN-γ (all from

Biolegend, San Diego, USA) were used according to the manufacturer's protocol. Absorbance at 570 nm was measured and subtracted from the absorbance at 450 nm using an Infinite 200 PRO plate-reader (TECAN, Männedorf, Switzerland). Standard curves were performed in duplicate.

2.14. Confocal microscopy

1.5×10^5 BMDC were incubated with Blue DND-22 LysoTracker (1:1000; Molecular Probes, Eugene, USA) in 300 µL complete BMDC medium without phenol red in Lab-Tek II 8-chambered coverglass 1.5 system (Nunc, Roskilde, Denmark). After 1 h, FITC-labeled particles (50.5 µg/ml) were added for an additional 4 h before live cell imaging by confocal microscopy (Zeiss, Oberkochen, Germany) at 20× and 60× magnification

2.15. In vitro T-cell proliferation

BMDC ($5x10^4$ cells/well) were cultured for 24 h with spider silk particles in the absence or presence of R848 (0.25 µg/ml) to induce BMDC maturation. Splenic OT-I $CD8^+$ T-cells were then negatively selected using a $CD8^+$ T-cell mouse isolation kit (Miltenyi Biotech, Bergisch Gladbach, Germany), stained with 5,6-carboxyfluorescein diacetate succinimidyl ester (CFSE; Biolegend, San Diego, USA) according to the manufacturer's protocol, and added to BMDC at 10^5 cells per well for 3 days. Cells were harvested for flow cytometry analysis, and the supernatant was stored at −20 °C for cytokine quantification. T-cell proliferation was determined using flow cytometry to assess the percentage of $CFSE^{low}$ cells within the $CD3^+CD8^+$ T-cell population.

2.16. Particle biodistribution

C57BL/6JRj mice were injected s.c. with 500 µg FITC-labeled C16-catSsub-OVAp in 100 µL PBS in the lower part of the right flank. After 24 h, lymphoid organs were isolated. The percentage of FITC+ cells was determined per organ and in defined immune cell populations of the draining lymph nodes: macrophages ($CD11c^-CD11b^+$), $CD11b^{low}$ dendritic cells ($CD11b^{low}CD11c^+$), $CD11b^{high}$ dendritic cells ($CD11b^{high}CD11c^+$) and other cells ($CD11c^-CD11b^-$).

2.17. In vivo T-cell proliferation

10^6 CFSE-labeled $CD8^+$ OT-I cells were adoptively transferred i.v. into C57BL/6JRj mice. 18 h later, mice were immunized s.c. in the right flank with 500 µg spider silk particles with or without R848 (25 µg) as adjuvant in 100 µL PBS. 3 days after immunization, inguinal draining lymph nodes were isolated for flow cytometry analysis. Proliferation was determined as above.

2.18. Statistical analysis

Fig. 1 was drawn with Origin 8 (OriginLab Corporation, Northampton, USA). Figs. 2–7 were drawn using GraphPad Prism version 6.0g (GraphPad Software, San Diego, USA). The statistical tests used are indicated in the figure legends. For cell culture experiments (Figs. 2–7), error bars indicate the standard error of the mean (SEM) of independent experiments performed on different days. Each experiment was performed in duplicate or triplicate. Statistical significance of multiple groups to the control group (untreated sample) was assessed using one-way ANOVA followed by Dunnett's multiple comparison test. Statistical significance between all groups was assessed using two-way ANOVA followed by Tukey's multiple comparison test (Fig. 5).

3. Results and discussion

The aim of this study was the development and formulation of a novel particulate delivery system to improve the induction of cytotoxic T-cell responses following peptide vaccination. To design a particulate peptide vaccine based on spider silk proteins, a MHC I-

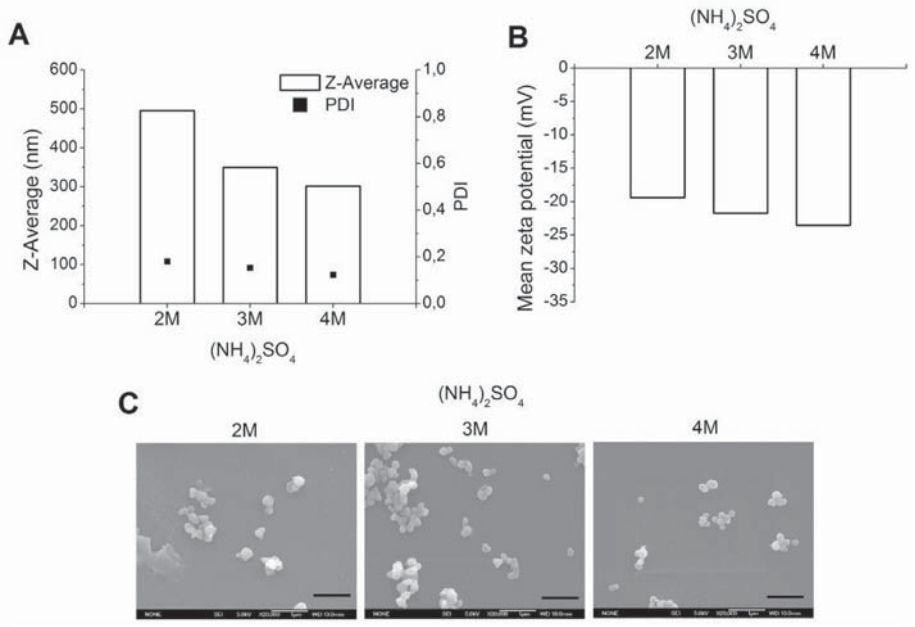

Fig. 1. Optimization of the spider silk particles synthesis. Properties of C16 spider silk particles after precipitation with ammonium sulfate solution ($(NH_4)_2SO_4$) at different ionic strengths at 1 mg/ml protein concentration and 50 ml/min flow rate. (A) Particle size given as the Z-average and the particle dispersity index (PDI). (B) Zeta potential of C16 particles after precipitation with different ionic strengths. Bars represent mean of three replicates. (C) SEM micrographs of C16 particles at a 20,000× magnification. The particles were dried under vacuum and carbon sputtered before imaging. Scale bar: 1 µm.

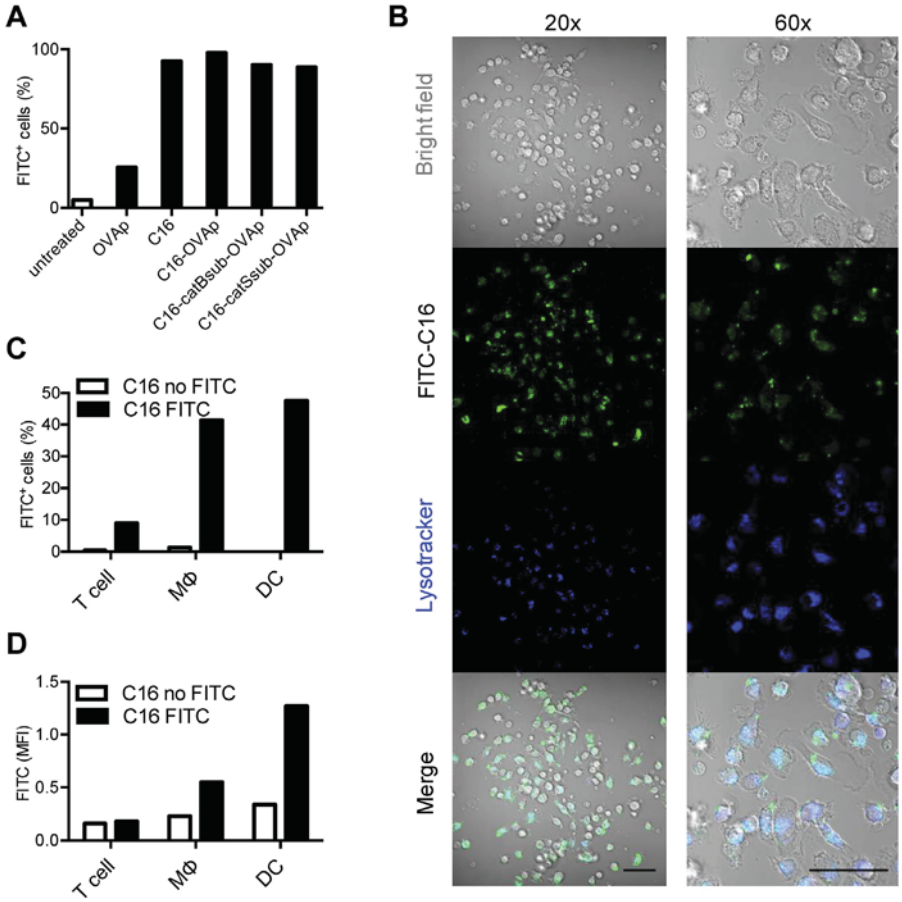

Fig. 2. Spider silk particles are preferentially taken up by dendritic cells. (A) BMDC were exposed to 50 μg/ml FITC-labeled spider silk particles (= 1 μg/ml OVA peptide) or FITC-labeled OVA peptide (OVAp; 1 μg/ml) for 24 h. Percentage of FITC-positive cells within BMDC population was determined by flow cytometry. Bars represent mean of 2 independent experiments (B) BMDC were incubated with LysoTracker for 1 h and FITC-labeled C16 particles for an additional 4 h before imaging by confocal microscopy. Live cell imaging at 20× and 60× magnification. Scale bar: 50 μm. (C–D) Freshly isolated splenocytes were cultured with FITC-labeled or unlabeled C16 particles for 4 h. Percentage of FITC-positive cells (C) and median fluorescent intensity (MFI) (D) was determined within T-cells, macrophages (MΦ) and dendritic cells (DC). One representative experiment of 3 independent experiments is shown.

restricted peptide from the model antigen ovalbumin, $OVA_{257-264}$, was fused to the C-terminus of a previously engineered spider silk protein, eADF4(C16) [32], using a cathepsin-cleavable linker. Four different recombinantly engineered proteins were used in this study: eADF4(C16) without modification, termed C16, the C16-ovalbumin peptide hybrid protein without linker (C16-OVAp), the hybrid protein with a cathepsin B substrate linker (C16-catBsub-OVAp) and the hybrid protein with a cathepsin S substrate linker (C16-catSsub-OVAp) (Fig. S1). Particles were prepared as previously described [33].

3.1. Preparation and characterization of hybrid spider silk-OVA peptide particles

As a first step, the impact of the OVA peptide addition to the engineered spider silk protein on the size and zeta potential of the particles was evaluated. The size of the newly designed C16-OVAp particles (average 369 nm) and the C16-catBsub-OVAp particles (386 nm) were comparable to that of C16 particles (363 nm). In contrast, the C16-catSsub-OVAp particles were significantly larger (510 nm) (Table S1).

In a small-scale optimization study conditions which give a more homogenous size range for all particle types were defined. Because the preparation of spider silk particles is based on salting out using kosmotropic ions according to the Hofmeister series [42], the effects of a change of the used salt solution for protein precipitation were evaluated first. At 2 M buffer strength, the change from potassium phosphate to ammonium sulfate had negligible effect on size (data not shown), but a trend towards smaller particles with increasing ionic strength of the ammonium sulfate solution was observed (Fig. 1A). The effect of both a decreased protein concentration (0.5 mg/ml instead of 1 mg/ml) and a decreased flow rate (25 ml/min instead of 50 ml/min) lowered the final particle size only marginally (data not shown). Zeta potential measurements of the spider silk particles showed slightly more negative values for the particles prepared with the higher molar ammonium sulfate solutions (Fig. 1B). Finally, SEM micrographs demonstrated that particles prepared in solutions with different ionic strengths were all round with a smooth and unimpaired surface (Fig. 1C).

To study the interactions of the different spider silk particles with immune cells, the following conditions (4 M ammonium sulfate solution, 1 mg/ml protein concentration, flow rate of 50 ml/min) were selected for the preparation of two endotoxin-free particle batches (below 0.24 EU/mg protein). All particle types were in a narrow size range between 241 nm and 325 nm and had a zeta potential between −22 mV and −29 mV (Table 1). In SEM, roundly shaped particles were visible without damage or fragments (Fig. S2). Spider silk particles from both preparation batches were used interchangeably for all further experiments without affecting the results. Worth noting is the stability of the particles when

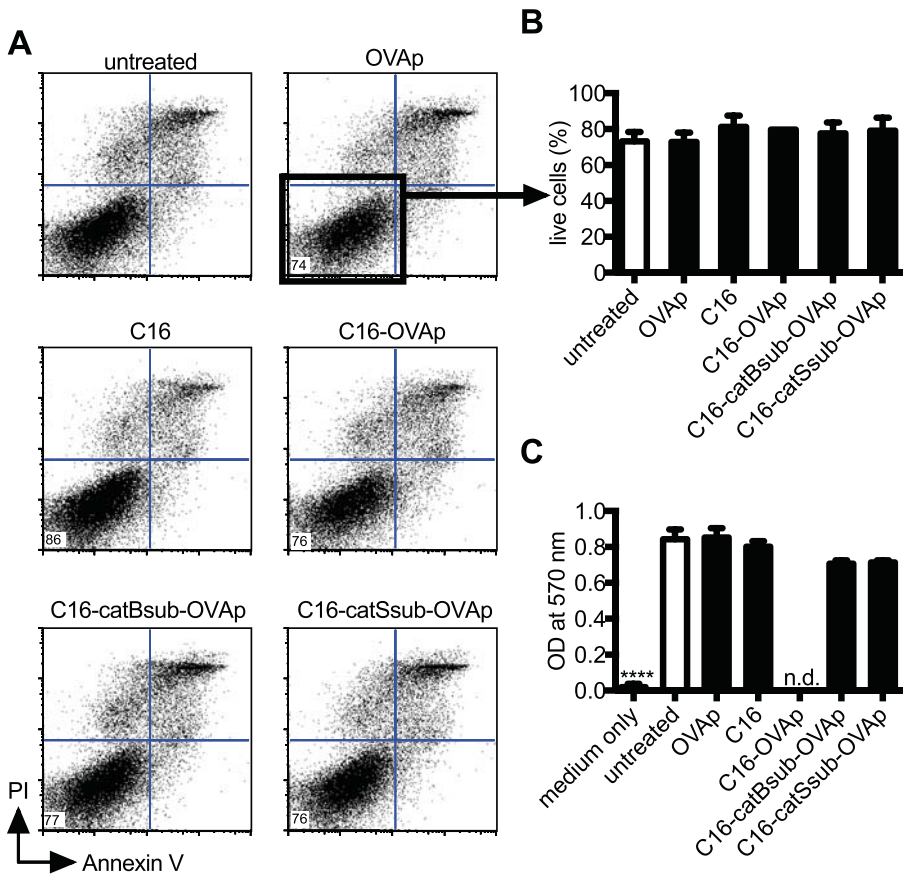

Fig. 3. Spider silk particles do not affect viability of dendritic cells. BMDC were cultured with engineered spider silk particles at 500 μg particles/ml (= 10 μg/ml OVA peptide) or OVA peptide (OVAp; 10 μg/ml). After 24 h, BMDC viability was assessed by flow cytometry (A and B) and MTT assay (C). (A) Representative dot plots for annexin V/propidium iodide staining. (B) Percentage of live cells (annexin V−/PI−, lower left quadrant). (C) Metabolic activity of BMDC measured by MTT assay of formazan production. n.d.: not done. (B and C) Bars represent mean ± SEM of 3 independent experiments (Panel B, C16-OVAp: mean of one experiment). Asterisks (****, $P \leq 0.0001$) indicate significant differences with untreated group using one-way ANOVA followed by Dunnett's multiple comparison test.

stored at 2–8 °C in highly purified water. Although formal stability studies were conducted for up to six months only with particles without the antigenic peptide [33], C16-OVAp particles both with and without cleavage site linkers showed excellent stability. Repetition of immunological assays shown in chapters 3.2 to 3.7 within a time period of 12 months did not change the outcome of the analyses.

To assess the capability of the two hybrid proteins containing a cathepsin cleavable linker sequence to serve as substrate, an enzymatic release test with cathepsin B and cathepsin S was conducted [35,36]. The amount of released peptides containing the OVA peptide sequence was evaluated by RP-HPLC analysis after incubation for 96 h at 37 °C (Fig. S3). The recombinant protein containing the cathepsin B cleavage site was poorly cleaved by cathepsin B, whereas the peptide containing the cathepsin S cleavage site was released upon exposure to cathepsin S. Antigen-presenting cells, such as macrophages and dendritic cells, display a high enzymatic activity of cathepsins B and S in the endosome [43,44], suggesting that the hybrid proteins could be readily cleaved at the designed substrate site after uptake into the endosome by these immune cell populations.

3.2. Spider silk particles are preferentially taken up by dendritic cells

To investigate whether the spider silk particles were taken up by dendritic cells, which are essential for the initiation of T-cell-mediated immune responses, a primary culture of dendritic cells differentiated from mouse bone marrow (bone marrow-derived dendritic cells, BMDC) was exposed to FITC-labeled particles or $OVA_{257-264}$ peptide. For all particle types tested, more than 90% of the BMDC were FITC-positive after 24 h exposure, whereas only 25% were positive after exposure to FITC-labeled OVA peptide (Fig. 2A). The uptake of the particles by BMDC was confirmed by confocal microscopy. Low magnification pictures showed that most of the cells were FITC-positive after incubation with FITC-labeled C16 particles (Fig. 2B left). In addition, a lysosomal staining (LysoTracker) was used to determine whether particles were localized in the lysosome of the cells, where cathepsins B and S are active. Indeed, larger magnification pictures highlight the co-localization of particles with lysosomes (Fig. 2B right). Similar results were obtained for all FITC-labeled particle types (Fig. S4).

To determine which immune cell population most efficiently took up the spider silk particles, we incubated freshly isolated mouse splenocytes, which contain a variety of different immune cell types, with FITC-labeled C16 particles (Fig. 2C). Only few T cells were positive for FITC, whereas over 40% of macrophages and 47% of dendritic cells were FITC-positive. Assessment of the median fluorescence intensity (MFI) showed that dendritic cells took up more particles than macrophages on a per-cell basis (Fig. 2D). Similar results were obtained for all formulations of the FITC-labeled particles (Fig. S5). Interestingly, dendritic cells showed a

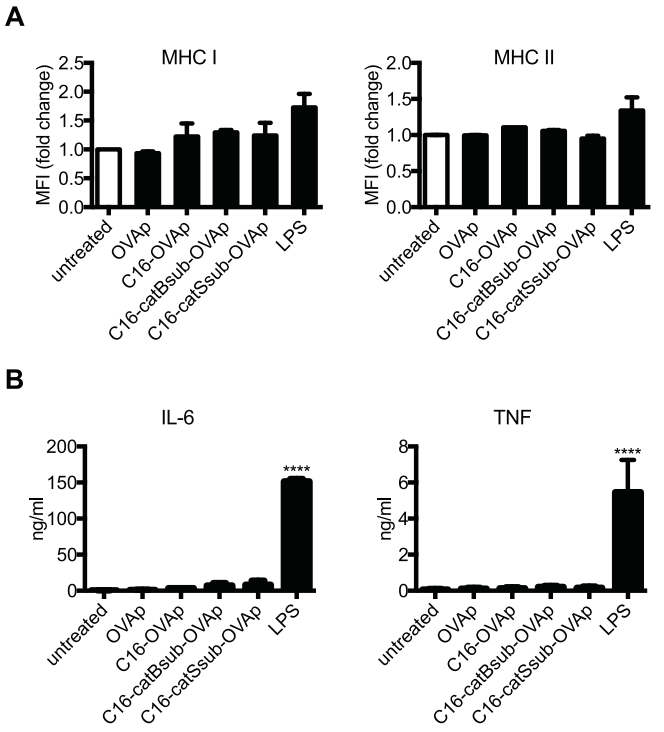

Fig. 4. Spider silk particles do not induce proinflammatory responses in dendritic cells. BMDC were cultured with 50 μg particles/ml (= 1 μg/ml OVA peptide) or OVA peptide alone (OVAp; 1 μg/ml). Lipopolysaccharide (LPS) (100 ng/ml) was used as positive control. After 24 h, BMDC were analyzed by flow cytometry, and supernatant was collected for cytokine quantification. (A) Median fluorescent intensity (MFI) of BMDC surface activation markers: fold change compared to untreated sample. (B) Quantification of cytokines in supernatant by ELISA. (A and B) Bars represent mean ± SEM of at least 3 independent experiments. Asterisks (****, $P \leq 0.0001$) indicate significant differences with untreated control group using one-way ANOVA followed by Dunnett's multiple comparison test.

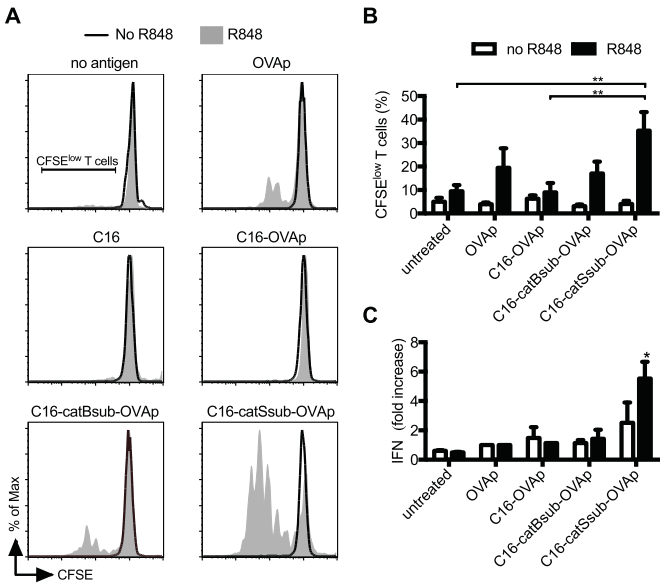

Fig. 5. Cathepsin S-cleavable hybrid spider particles induce a strong cytotoxic T-cell proliferation in vitro. BMDC were cultured with 50 μg particles/ml (= 1 μg/ml OVA peptide) or OVA peptide alone (OVAp; 1 μg/ml) with or without R848 (0.25 μg/ml) for 24 h. CFSE-labeled OVAp-specific CD8 T-cells were added for 3 days before analysis of T-cell proliferation by flow cytometry. (A) Histograms of CFSE dilution from one representative experiment. (B) Percentage of $CFSE^{low}$ proliferating cells within the T-cell population ($CD3^+CD8^+$). (C) IFN-γ quantification in the supernatant: fold increase compared to OVA peptide. (B and C) Bars represent mean ± SEM of 3 independent experiments. Asterisks (*, $P \leq 0.05$; **, $P \leq 0.01$) indicate significant differences between groups using two-way ANOVA followed by Tukey's multiple comparison test.

better uptake even if they generally show less phagocytic activity than macrophages. The difference in uptake between cell types may be explained by the fact that dendritic cells preferentially take up virus-sized particles (below 500 nm, as was the case for the spider silk particles) whereas macrophages preferentially take up larger particles (0.5–5 μm) [45]. Moreover, slightly negative particles might be taken up by micropinocytosis in dendritic cells [46]. In a study comparing the uptake of PLGA particles with a size ranging from 300 nm to 17 μm, the 300 nm particles were most efficiently taken up by dendritic cells and induced the highest T-cell responses when used as vaccine delivery system [47]. Taken together, we show that all spider silk particles tested, with a size of approximately 300 nm and a zeta-potential of approximately −25 mV, are efficiently taken up by dendritic cells and macrophages.

3.3. Spider silk particles do not affect viability of dendritic cells

It is well described that particles can affect the viability of immune cells [48]. To determine whether the uptake of hybrid spider silk particles by dendritic cells can lead to cell death, BMDC were exposed for 24 h to a particle concentration 10 times higher than the concentration used for other in vitro experiments. Cell death was measured by flow cytometry using annexin V and propidium iodide (PI) staining to differentiate between apoptotic cells and dead cells. None of the spider silk particles tested affected the percentage of live BMDC (annexin V/PI double-negative cells) (Fig. 3A and B). These results were confirmed by an independent metabolic assay, the 3-(4,5-dimethylthiazol-2-yl)-2,5-diphenyltetrazolium bromide assay (MTT assay, Fig. 3C). This method, which reflects the mitochondrial activity of cells, is frequently used as high-throughput screening assay to determine toxicity of compounds [49]. No impairment of the metabolic activity of BMDC was observed for any of the spider silk particles tested. Thus, using two independent methods, we demonstrated that hybrid spider silk particles do not induce apoptotic or necrotic cell death in BMDC. These results correlate with previous studies demonstrating the biocompatibility of native spider silk particles [50].

3.4. Spider silk particles do not induce proinflammatory responses in dendritic cells

Because unspecific dendritic cell maturation may lead to generalized inflammatory responses, we investigated whether the particles were pro-inflammatory in themselves. BMDC were incubated with spider silk particles for 24 h before testing for signs of dendritic cell maturation, such as the up-regulation of the antigen-presenting molecules and of the co-stimulatory factors on the cell surface. Lipopolysaccharide, a Toll-like receptor 4 agonist, was used as positive control to induce BMDC maturation [51]. None of the particle types induced a significant up-regulation of antigen-presenting molecules (MCH I and MHC II) on BMDC (Fig. 4A) nor increased the density of the co-stimulatory factors (CD80 and CD86) (data not shown). Once activated, dendritic cells secrete pro-inflammatory cytokines such as interleukine-6 (IL-6) and tumor necrosis factor alpha (TNF-α) in order to recruit and activate other immune cells. To determine whether spider silk particles induce the secretion of these pro-inflammatory cytokines, the culture supernatant was collected after 24 h incubation of particles with

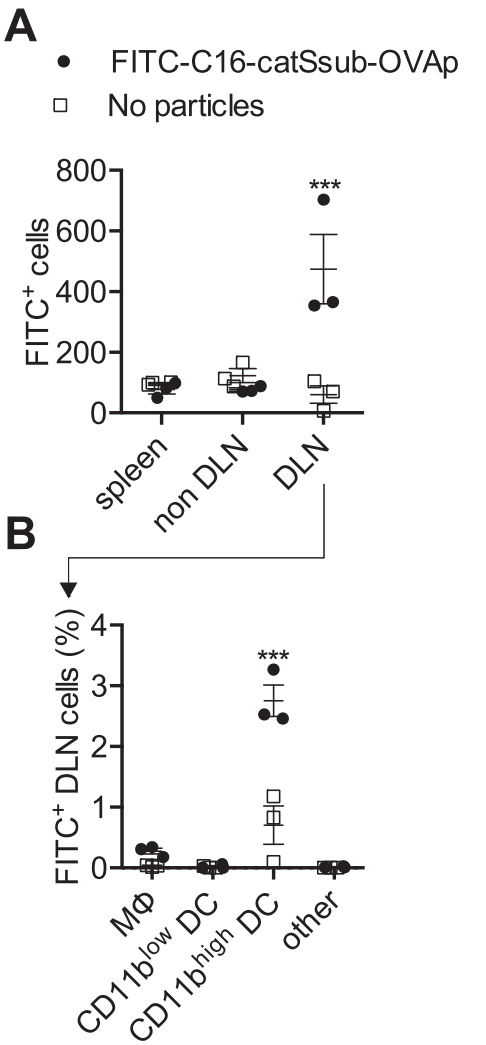

Fig. 6. Cathepsin S-cleavable hybrid spider silk particles accumulate in the draining lymph nodes. FITC-labeled C16-catSsub-OVAp particles were injected s.c. into the right flank of 3 mice. 24 h after injection, the spleen, contralateral non-draining inguinal lymph nodes (non DLN) and draining ipsilateral inguinal lymph nodes (DLN) were isolated for flow cytometry analysis. (A) Number of FITC+ cells in the different organs. (B) Percentage of FITC+ cells within defined immune cell populations. Each dot represents one mouse. Bars represent mean ± SEM. Asterisks (***, $P \leq 0.001$) indicate significant differences when comparing particle-treated mice with PBS-treated mice using two-way ANOVA followed by Bonferroni's multiple comparison test.

BMDC and assessed by ELISA. None of the spider silk particles induced a significant secretion of these cytokines (Fig. 4B). Thus, the hybrid spider silk particles showed no intrinsic pro-inflammatory activity and did not lead to unspecific immune activation in vitro.

3.5. Cathepsin S-cleavable hybrid spider silk particles induce a strong cytotoxic T-cell proliferation in vitro

To induce an effective cytotoxic T-cell response to the model antigenic peptide $OVA_{257-264}$, the OVA peptide must be cleaved from the spider silk protein and cross-presented by antigen-presenting cells in an MHC-class I-restricted manner [52,53]. Cross-presentation can further be supported by the activity of cathepsin S [54]. To determine whether the hybrid spider silk particles could be processed and the OVA peptide efficiently presented, a BMDC-induced T-cell proliferation assay using OVA-

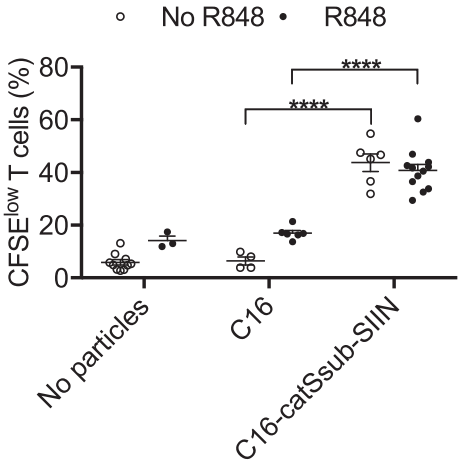

Fig. 7. Cathepsin S-cleavable hybrid spider particles induce strong cytotoxic T-cell responses in vivo. CFSE-labeled $CD8^+$ OT-I cells were injected i.v. into mice. 18 h later, mice were vaccinated with spider silk particles (500 μg per mouse). R848 (25 μg) was used as adjuvant. 3 days after vaccination, draining lymph nodes were isolated for flow cytometry analysis to determine the proliferation of $CD3^+CD8^+$ CFSE-labeled OT-I cells. Each dot represents one mouse. Bars represent mean ± SEM. Asterisks (****, $P \leq 0.0001$) indicate significant differences with R848-treated control group using one-way ANOVA followed by Dunnett's multiple comparison test.

specific cytotoxic T cells (OT-I T-cells) [55] was performed. BMDC were incubated with spider silk hybrid particles as antigen donor and with resiquimod (R848) as adjuvant to induce BMDC maturation. After 24 h, CFSE-labeled OT-I T cells were added to the culture and T-cell proliferation was assessed 3 days later by measuring CFSE dilution, where $CFSE^{low}$ cells represent divided cells. No T-cell proliferation was induced by BMDC loaded with C16-OVAp particles (Fig. 5A and B). Little T-cell proliferation was seen after co-culture with BMDC loaded with C16-catBsub-OVAp particles. In contrast, BMDC exposed to C16-catSsub-OVAp induced a strong T-cell proliferation that was much higher than with BMDC exposed to free OVA peptide. This high proliferation was associated with higher levels of IFNγ secretion (Fig. 5C). Thus, particles prepared from hybrid proteins with a cathepsin S-cleavable linker induced the strongest priming of antigen-specific T cells. These particles were selected for further in vivo investigations in mice.

3.6. Cathepsin S-cleavable hybrid spider silk particles accumulate in the draining lymph nodes

As the activation of cytotoxic T cells by dendritic cells occurs in lymph nodes, it is essential that the antigen-bearing particles reach these organs. To assess whether this was the case, the biodistribution of FITC-labeled C16-catSsub-OVAp particles was analyzed following their subcutaneous injection into the flank of mice. 24 h after injection, the spleen, contralateral non-draining lymph nodes and ipsilateral draining lymph nodes were isolated for flow cytometry detection of FITC fluorescence. Spider silk particles were clearly detected in the draining lymph nodes but not in non-draining lymph nodes nor in the spleen (Fig. 6A). Importantly, none of the treated mice showed any sign of toxicity during the experiment.

Nanoparticles may reach the draining lymph nodes by one of two mechanisms: they can be borne passively to the lymph nodes via the lymph and be trapped there by resident macrophages, or be taken up by dendritic cells at the injection site and actively transported to the lymph node [56]. Because spider silk particles are larger than 200 nm, they are expected to be taken up by dendritic cells at the site of injection [57]. To distinguish between these two

Table 1
Properties of the engineered spider silk particles after endotoxin-free preparation. Particle size given as Z-average, particle dispersity index (PDI) and zeta potential. Mean ± SD. Particles were prepared at 80 °C at a protein concentration of 1 mg/ml. For some particle types two batches were prepared.

	Batch	Z-average (nm)	PDI	Zeta potential (mV)
C16	1	252.0 ± 5.8	0.069 ± 0.012	−27.0 ± 1.3
	2	242.8 ± 2.9	0.091 ± 0.045	−24.1 ± 1.0
C16-OVAp	1	253.6 ± 3.0	0.096 ± 0.007	−25.7 ± 1.5
C16-CatBsub-OVAp	1	241.1 ± 3.3	0.062 ± 0.019	−28.8 ± 1.7
	2	249.0 ± 1.9	0.080 ± 0.023	−26.9 ± 1.0
C16-CatSsub-OVAp	1	283.1 ± 4.4	0.090 ± 0.024	−28.1 ± 1-6
	2	250.7 ± 4.2	0.111 ± 0.036	−25.3 ± 1.2
FITC-C16	1	270.6 ± 0.8	0.055 ± 0.024	−26.3 ± 1.2
FITC-C16-OVAp	1	325.0 ± 8.7	0.120 ± 0.031	−22.2 ± 1.5
FITC-C16-CatBsub-OVAp	1	285.6 ± 3.3	0.101 ± 0.008	−27.4 ± 1.4
FITC-C16-CatSsub-OVAp	1	318.2 ± 3.6	0.129 ± 0.024	−27.5 ± 1.2
	2	245.5 ± 4.1	0.090 ± 0.027	−25.8 ± 0.9

transport mechanisms, the cell population that was positive for spider silk particles in the lymph nodes was determined. Neither macrophages nor $CD11b^{low}$ dendritic cells were found to be significantly FITC-positive (Fig. 6B). In contrast, $CD11b^{high}$ dendritic cells were clearly positive for FITC, indicating that this cell population had taken up FITC-labeled C16-catSsub-OVAp particles. This data correlated with the in vitro uptake assay demonstrating that dendritic cells were the main population to take up spider silk particles (Fig. 6). It is probable that the particles were taken up by classical dermal dendritic cells, which are $CD11b^{high}$, rather than $CD103^{+}$ dendritic cells, which are $CD11b^{low}$ [58]. Importantly, dermal dendritic cells can prime cytotoxic T-cell responses [59–61].

3.7. Cathepsin S-cleavable hybrid spider silk particles induce strong T-cell responses in mice

In order to examine the potential of spider silk-OVA peptide particles to induce a cytotoxic T-cell response, an in vivo T-cell proliferation assay was performed. First CFSE-labeled OT-I T-cells were injected into recipient wild-type mice. One day later, mice were vaccinated using the cathepsin S-cleavable hybrid particles as antigen carrier and resiquimod (R848) as adjuvant to induce dendritic cell maturation. Three days after vaccination, the draining lymph nodes of the treated mice were isolated for quantification of OVAp-specific T-cell proliferation. C16-catSsub-OVAp were highly efficient in inducing antigen-specific proliferation of cytotoxic T cells, whereas C16 particles without OVA peptide were not (Fig. 7). Importantly, T-cell proliferation induced by cathepsin S-cleavable particles was just as strong in the absence of R848 as adjuvant.

This is of importance, because other carrier systems usually require co-administration of a direct immunostimulatory adjuvant such as R848 to induce immune responses. For example, PLGA particles in the size range between 350 and 410 nm showed much greater effect when co-administered with an immunostimulatory adjuvant [62]. Unfortunately, a high burst release of the adjuvant after administration is commonly observed when PLGA particles are used [63]. When multilamellar liposomes with a comparable size to the spider silk-OVA peptide particles were used as delivery system for protein antigens, they induced more efficient T-cell proliferation in presence of a direct immunostimulatory adjuvant [64]. This effect was even greater when the adjuvant was encapsulated with the antigen inside the carrier. However, the preparation of these multilamellar liposomes requires an additional cross-linking step during preparation, which bears the potential risk of toxic cross-linking residues in the final product.

4. Conclusions

Cellular immunity is of major importance for protection against certain infectious diseases and in cancer. Here, we demonstrate the ability of engineered spider silk particles to function as peptide vaccine delivery system and to induce cytotoxic T-cell proliferation in the draining lymph nodes of mice. Importantly, this effect was seen even in the absence of adjuvant, although the particles alone were not pro-inflammatory and did not induce unspecific immune responses. Our results also demonstrate the high stability of the particles, allowing for storage for over a year and heat sterilization without losing their immune functionality. Moreover, particles from two fully independent batches led to comparable in vivo results demonstrating a robust manufacturing process. Thus, a sound basis for a protein-based all-in-one vaccination system is set, where spider silk particles serve as particulate vaccine carriers for customized peptide epitopes. The presented findings can be the basis for future studies to screen additional linker sequences and more epitopes. The following studies should also focus on encapsulation of an adjuvant within the particles to possibly enhance the effect of the antigen presentation, allowing for a reduction of antigen per dose.

Competing interest statement

The authors confirm that there are no known conflicts of interest associated with this publication and there has been no significant financial support for this work that could have influenced its outcome.

Data availability statement

The raw/processed data required to reproduce these findings cannot be shared at this time due to a pending patent application.

Acknowledgements

This work was supported by a grant from the Federal Ministry of Education and Research, Germany (grant number: 13N11341 GW; grant number: 13N11340 TS), the National Center of Competence in Research (NCCR) for Bio-Inspired Materials to CB and the Swiss National Science Foundation grants 156372 and 156871 to CB. We thank C. Minke (Ludwig-Maximilians-University Munich, Department of Chemistry) for assistance with scanning electron microscopy and A. Oberson and J.Widmer (both from University of Fribourg, Department of Medicine) for assistance with cell-based experiments.

Appendix A. Supplementary data

Supplementary data related to this article can be found at https://doi.org/10.1016/j.biomaterials.2018.04.008.

References

[1] K.T. Gause, A.K. Wheatley, J. Cui, Y. Yan, S.J. Kent, F. Caruso, Immunological principles guiding the rational design of particles for vaccine delivery, ACS Nano 11 (1) (2017) 54–68.
[2] V. Appay, D.C. Douek, D.A. Price, CD8+ T cell efficacy in vaccination and disease, Nat. Med. 14 (6) (2008) 623–628.
[3] R.A. Seder, P.A. Darrah, M. Roederer, T-cell quality in memory and protection: implications for vaccine design, Nat. Rev. Immunol. 8 (4) (2008) 247–258.
[4] N.P. Restifo, M.E. Dudley, S.A. Rosenberg, Adoptive immunotherapy for cancer: harnessing the T cell response, Nat. Rev. Immunol. 12 (4) (2012) 269–281.
[5] R.A. Seder, A.V. Hill, Vaccines against intracellular infections requiring cellular immunity, Nature 406 (6797) (2000) 793–798.
[6] J. Banchereau, F. Briere, C. Caux, J. Davoust, S. Lebecque, Y.J. Liu, B. Pulendran, K. Palucka, Immunobiology of dendritic cells, Annu. Rev. Immunol. 18 (2000) 767–811.
[7] E.S. Trombetta, I. Mellman, Cell biology of antigen processing in vitro and in vivo, Annu. Rev. Immunol. 23 (2005) 975–1028.
[8] R.M. Zinkernagel, Restriction by H-2 gene complex of transfer of cell-mediated immunity to Listeria monocytogenes, Nature 251 (5472) (1974) 230–233.
[9] N. Romani, S. Koide, M. Crowley, M. Witmer-Pack, A.M. Livingstone, C.G. Fathman, K. Inaba, R.M. Steinman, Presentation of exogenous protein antigens by dendritic cells to T cell clones. Intact protein is presented best by immature, epidermal Langerhans cells, J. Exp. Med. 169 (3) (1989) 1169–1178.
[10] K. Hoebe, E. Janssen, B. Beutler, The interface between innate and adaptive immunity, Nat Immunol. 5 (10) (2004) 971–974.
[11] C. Munz, Live long and prosper for antigen cross-presentation, Immunity 43 (6) (2015) 1028–1030.
[12] D. Palliser, H. Ploegh, M. Boes, Myeloid differentiation factor 88 is required for cross-priming in vivo, J. Immunol. 172 (6) (2004) 3415–3421.
[13] G.J. Randolph, V. Angeli, M.A. Swartz, Dendritic-cell trafficking to lymph nodes through lymphatic vessels, Nat. Rev. Immunol. 5 (8) (2005) 617–628.
[14] J. Banchereau, R.M. Steinman, Dendritic cells and the control of immunity, Nature 392 (6673) (1998) 245–252.
[15] K. Falk, O. Rotzschke, S. Stevanovic, G. Jung, H.G. Rammensee, Allele-specific motifs revealed by sequencing of self-peptides eluted from MHC molecules, Nature 351 (6324) (1991) 290–296.
[16] C.L. Slingluff Jr., The present and future of peptide vaccines for cancer: single or multiple, long or short, alone or in combination? Cancer J. 17 (5) (2011) 343–350.
[17] R.E. Toes, R.J. Blom, R. Offringa, W.M. Kast, C.J. Melief, Enhanced tumor outgrowth after peptide vaccination. Functional deletion of tumor-specific CTL induced by peptide vaccination can lead to the inability to reject tumors, J. Immunol. 156 (10) (1996) 3911–3918.
[18] R.E. Toes, R. Offringa, R.J. Blom, C.J. Melief, W.M. Kast, Peptide vaccination can lead to enhanced tumor growth through specific T-cell tolerance induction, Proc. Natl. Acad. Sci. U. S. A. 93 (15) (1996) 7855–7860.
[19] S.H. van der Burg, M.J. Visseren, R.M. Brandt, W.M. Kast, C.J. Melief, Immunogenicity of peptides bound to MHC class I molecules depends on the MHC-peptide complex stability, J. Immunol. 156 (9) (1996) 3308–3314.
[20] D.H. Busch, E.G. Pamer, MHC class I/peptide stability: implications for immunodominance, in vitro proliferation, and diversity of responding CTL, J. Immunol. 160 (9) (1998) 4441–4448.
[21] E. Ingulli, D.R. Ulman, M.M. Lucido, M.K. Jenkins, In situ analysis reveals physical interactions between CD11b+ dendritic cells and antigen-specific CD4 T cells after subcutaneous injection of antigen, J. Immunol. 169 (5) (2002) 2247–2252.
[22] D. Boraschi, P. Italiani, From antigen delivery system to adjuvanticy: the board application of nanoparticles in vaccinology, Vaccines 3 (4) (2015) 930–939.
[23] S. Jung, D. Unutmaz, P. Wong, G. Sano, K. De los Santos, T. Sparwasser, S. Wu, S. Vuthoori, K. Ko, F. Zavala, E.G. Pamer, D.R. Littman, R.A. Lang, In vivo depletion of CD11c+ dendritic cells abrogates priming of CD8+ T cells by exogenous cell-associated antigens, Immunity 17 (2) (2002) 211–220.
[24] M.O. Oyewumi, A. Kumar, Z. Cui, Nano-microparticles as immune adjuvants: correlating particle sizes and the resultant immune responses, Expert Rev. Vaccines 9 (9) (2010) 1095–1107.
[25] E.B. Lindblad, Aluminium compounds for use in vaccines, Immunol. Cell Biol. 82 (5) (2004) 497–505.
[26] M. Singh, A. Chakrapani, D. O'Hagan, Nanoparticles and microparticles as vaccine-delivery systems, Expert Rev. Vaccines 6 (5) (2007) 797–808.
[27] G.F. Walker, C. Fella, J. Pelisek, J. Fahrmeir, S. Boeckle, M. Ogris, E. Wagner, Toward synthetic viruses: endosomal pH-triggered deshielding of targeted polyplexes greatly enhances gene transfer in vitro and in vivo, Mol. Ther. 11 (3) (2005) 418–425.
[28] P.H. Zeplin, N.C. Maksimovikj, M.C. Jordan, J. Nickel, G. Lang, A.H. Leimer, L. Römer, T. Scheibel, Spider silk coatings as a bioshield to reduce periprosthetic fibrous capsule formation, Adv. Funct. Mater. 24 (18) (2014) 2658–2666.
[29] A. Leal-Egana, T. Scheibel, Silk-based materials for biomedical applications, Biotechnol. Appl. Biochem. 55 (3) (2010) 155–167.
[30] K. Spieß, S. Wohlrab, T. Scheibel, Structural characterization and functionalization of engineered spider silk films, Soft Matter 6 (17) (2010) 4168–4174.
[31] S. Wohlrab, S. Muller, A. Schmidt, S. Neubauer, H. Kessler, A. Leal-Egana, T. Scheibel, Cell adhesion and proliferation on RGD-modified recombinant spider silk proteins, Biomaterials 33 (28) (2012) 6650–6659.
[32] D. Huemmerich, C.W. Helsen, S. Quedzuweit, J. Oschmann, R. Rudolph, T. Scheibel, Primary structure elements of spider dragline silks and their contribution to protein solubility, Biochemistry 43 (42) (2004) 13604–13612.
[33] M. Hofer, G. Winter, J. Myschik, Recombinant spider silk particles for controlled delivery of protein drugs, Biomaterials 33 (5) (2012) 1554–1562.
[34] M. Lucke, G. Winter, J. Engert, The effect of steam sterilization on recombinant spider silk particles, Int. J. Pharm. 481 (1–2) (2015) 125–131.
[35] S.M. Ogbomo, W. Shi, N.K. Wagh, Z. Zhou, S.K. Brusnahan, J.C. Garrison, 177Lu-labeled HPMA copolymers utilizing cathepsin B and S cleavable linkers: synthesis, characterization and preliminary in vivo investigation in a pancreatic cancer model, Nucl. Med. Biol. 40 (5) (2013) 606–617.
[36] J.J. Peterson, C.F. Meares, Enzymatic cleavage of peptide-linked radiolabels from immunoconjugates, Bioconjugate Chem. 10 (4) (1999) 553–557.
[37] R. Duncan, L.W. Seymour, K.B. O'Hare, P.A. Flanagan, S. Wedge, I.C. Hume, K. Ulbrich, J. Strohalm, V. Subr, F. Spreafico, Preclinical evaluation of polymer-bound doxorubicin, J Control Release 19 (1992) 331–346.
[38] H. Soyez, E. Schacht, S. Vanderkerken, The crucial role of spacer groups in macromolecular prodrug design, Adv. Drug Deliv. Rev. 21 (2) (1996) 81–106.
[39] A. Lammel, M. Schwab, M. Hofer, G. Winter, T. Scheibel, Recombinant spider silk particles as drug delivery vehicles, Biomaterials 32 (8) (2011) 2233–2240.
[40] C. Bourquin, C. Hotz, D. Noerenberg, A. Voelkl, S. Heidegger, L.C. Roetzer, B. Storch, N. Sandholzer, C. Wurzenberger, D. Anz, S. Endres, Systemic cancer therapy with a small molecule agonist of toll-like receptor 7 can be improved by circumventing TLR tolerance, Cancer Res. 71 (15) (2011) 5123–5133.
[41] I. Mottas, A. Milosevic, A. Petri-Fink, B. Rothen-Rutishauser, C. Bourquin, A rapid screening method to evaluate the impact of nanoparticles on macrophages, Nanoscale 9 (7) (2017) 2492–2504.
[42] Y. Zhang, P.S. Cremer, Interactions between macromolecules and ions: the Hofmeister series, Curr. Opin. Chem. Biol. 10 (6) (2006) 658–663.
[43] R.J. Riese, R.N. Mitchell, J.A. Villadangos, G.P. Shi, J.T. Palmer, E.R. Karp, G.T. De Sanctis, H.L. Ploegh, H.A. Chapman, Cathepsin S activity regulates antigen presentation and immunity, J. Clin. Investig. 101 (11) (1998) 2351–2363.
[44] L.C. Hsing, A.Y. Rudensky, The lysosomal cysteine proteases in MHC class II antigen presentation, Immunol. Rev. 207 (2005) 229–241.
[45] C. Foged, B. Brodin, S. Frokjaer, A. Sundblad, Particle size and surface charge affect particle uptake by human dendritic cells in an in vitro model, Int. J. Pharm. 298 (2) (2005) 315–322.
[46] L.M. Kranz, M. Diken, H. Haas, S. Kreiter, C. Loquai, K.C. Reuter, M. Meng, D. Fritz, F. Vascotto, H. Hefesha, C. Grunwitz, M. Vormehr, Y. Hüsemann, A. Selmi, A.N. Kuhn, J. Buck, E. Derhovanessian, R. Rae, S. Attig, J. Diekmann, R.A. Jabulowsky, S. Heesch, J. Hassel, P. Langguth, S. Grabbe, C. Huber, Ö. Türeci, U. Sahin, Systemic RNA delivery to dendritic cells exploits antiviral defence for cancer immunotherapy, Nature 534 (7607) (2016) 396–401.
[47] V.B. Joshi, S.M. Geary, A.K. Salem, Biodegradable particles as vaccine delivery systems: size matters, AAPS J. 15 (1) (2013) 85–94.
[48] M.A. Dobrovolskaia, S.E. McNeil, Understanding the correlation between in vitro and in vivo immunotoxicity tests for nanomedicines, J Control Release 172 (2) (2013) 456–466.
[49] T. Mosmann, Rapid colorimetric assay for cellular growth and survival: application to proliferation and cytotoxicity assays, J. Immunol. Met. 65 (1–2) (1983) 55–63.
[50] M.B. Schierling, E. Doblhofer, T. Scheibel, Cellular uptake of drug loaded spider silk particles, Biomater. Sci. 4 (10) (2016) 1515–1523.
[51] F. Granucci, E. Ferrero, M. Foti, D. Aggujaro, K. Vettoretto, P. Ricciardi-Castagnoli, Early events in dendritic cell maturation induced by LPS, Microbes Infect. 1 (13) (1999) 1079–1084.
[52] H. Shen, A.L. Ackerman, V. Cody, A. Giodini, E.R. Hinson, P. Cresswell, R.L. Edelson, W.M. Saltzman, D.J. Hanlon, Enhanced and prolonged cross-presentation following endosomal escape of exogenous antigens encapsulated in biodegradable nanoparticles, Immunology 117 (1) (2006) 78–88.
[53] O.P. Joffre, E. Segura, A. Savina, S. Amigorena, Cross-presentation by dendritic cells, Nat. Rev. Immunol. 12 (8) (2012) 557–569.
[54] L. Shen, L.J. Sigal, M. Boes, K.L. Rock, Important role of cathepsin S in generating peptides for TAP-independent MHC class I crosspresentation in vivo, Immunity 21 (2) (2004) 155–165.
[55] S.R. Clarke, M. Barnden, C. Kurts, F.R. Carbone, J.F. Miller, W.R. Heath, Characterization of the ovalbumin-specific TCR transgenic line OT-I: MHC elements for positive and negative selection, Immunol. Cell Biol. 78 (2) (2000) 110–117.
[56] D.J. Irvine, M.A. Swartz, G.L. Szeto, Engineering synthetic vaccines using cues from natural immunity, Nat. Mater. 12 (11) (2013) 978–990.
[57] V. Manolova, A. Flace, M. Bauer, K. Schwarz, P. Saudan, M.F. Bachmann, Nanoparticles target distinct dendritic cell populations according to their size, Eur. J. Immunol. 38 (5) (2008) 1404–1413.
[58] W.R. Heath, F.R. Carbone, Dendritic cell subsets in primary and secondary T cell responses at body surfaces, Nat. Immunol. 10 (12) (2009) 1237–1244.
[59] R.S. Allan, C.M. Smith, G.T. Belz, A.L. van Lint, L.M. Wakim, W.R. Heath,

F.R. Carbone, Epidermal viral immunity induced by CD8alpha+ dendritic cells but not by Langerhans cells, Science 301 (5641) (2003) 1925–1928.
[60] M.V. Lukens, D. Kruijsen, F.E. Coenjaerts, J.L. Kimpen, G.M. van Bleek, Respiratory syncytial virus-induced activation and migration of respiratory dendritic cells and subsequent antigen presentation in the lung-draining lymph node, J. Virol. 83 (14) (2009) 7235–7243.
[61] T.S. Kim, T.J. Braciale, Respiratory dendritic cell subsets differ in their capacity to support the induction of virus-specific cytotoxic CD8+ T cell responses, PLoS One 4 (1) (2009), e4204.
[62] S. Hamdy, O. Molavi, Z. Ma, A. Haddadi, A. Alshamsan, Z. Gobti, S. Elhasi, J. Samuel, A. Lavasanifar, Co-delivery of cancer-associated antigen and Toll-like receptor 4 ligand in PLGA nanoparticles induces potent CD8+ T cell-mediated anti-tumor immunity, Vaccine 26 (39) (2008) 5046–5057.
[63] S.D. Allison, Effect of structural relaxation on the preparation and drug release behavior of poly(lactic-co-glycolic)acid microparticle drug delivery systems, J. Pharm. Sci. 97 (6) (2008) 2022–2035.
[64] J.J. Moon, H. Suh, A. Bershteyn, M.T. Stephan, H. Liu, B. Huang, M. Sohail, S. Luo, S.H. Um, H. Khant, J.T. Goodwin, J. Ramos, W. Chiu, D.J. Irvine, Interbilayer-crosslinked multilamellar vesicles as synthetic vaccines for potent humoral and cellular immune responses, Nat. Mater. 10 (3) (2011) 243–251.